ISSN 0036-0244, Russian Journal of Physical Chemistry A, 2018, Vol. 92, No. 3, pp. 475–481. © Pleiades Publishing, Ltd., 2018.

PHYSICAL CHEMISTRY OF SOLUTIONS

Phase Diagram of Quaternary System $NaBr-KBr-CaBr_2-H_2O$ at 323 K[1]

Rui-Zhi Cui, Wei Wang, Lei Yang, and Shi-Hua Sang*

College of Materials and Chemistry and Chemical Engineering, Chengdu University of Technology, Chengdu, 610059 P. R. China
Mineral Resources Chemistry Key Laboratory of Sichuan Higher Education Institutions, Chengdu, 610059 P. R. China
**e-mail: sangshihua@sina.com.cn, sangsh@cdut.edu.cn*

Received October 31, 2016

Abstract—The phase equilibria in the system $NaBr-KBr-CaBr_2-H_2O$ at 323 K were studied using the isothermal dissolution equilibrium method. Using the experimental solubilities of salts data, phase diagram was constructed. The phase diagram have two invariant points, five univariant curves, and four crystallization fields. The equilibrium solid phases in the system are NaBr, $NaBr \cdot 2H_2O$, KBr, and $CaBr_2 \cdot 4H_2O$. The solubilities of salts in the system at 323 K were calculated by Pitzer's equation. There is shown that the calculated solubilities agree well with experimental data.

Keywords: underground brine, phase equilibrium, solubility, Pitzer's equation, bromide

DOI: 10.1134/S003602441803024X

INTRODUCTION

The brine discovered in the west of Sichuan Basin contains high concentration of potassium and borate. Its salinity is average up to 377 g L^{-1}, and this brine is weakly acidic with pH value of 6.18. In addition to K^+, B^{3+}, the brine still has some useful components such as Br^-, I^-, Li^+, Sr^{2+}, etc., and all of them can reach or exceed the industrial index. Potassium concentration is up to 53.3 g L^{-1}, which is far higher than Qarhan Salt Lake brine (12.1 g L^{-1}) and Zabuye Salt Lake brine (27.0 g L^{-1}). Boron content appears abnormaly high, up to 4994 mg L^{-1}. In particular, the bromine content is also as high as 2533 mg L^{-1}. It has become the rare liquid mineral resources in the world. It will have great social and economic value by development and utilization the underground brine resources [1, 2] Our research work focuses on the phase equilibria of the Western Sichuan Basin brine-salt system from normal to high temperatures. The underground gasfield brines in Western Sichuan Basin can be simplified as six-component brine system $Na-K-Cl-Br-SO_4-B_4O_7-H_2O$. Generally speaking, multi-temperature phase diagrams are very important for the exploitation of liquid mineral resources. Systematic research of the salt systems such as $KBr-K_2B_4O_7-H_2O$ at 298, 323, 348, and 373 K [3–6], quaternary system $KCl-K_2SO_4-K_2B_4O_7-H_2O$ and $NaBr-KBr-CaBr_2-H_2O$ at 298 K [7–9], and quinary system Na^+, K^+//Cl^-, Br^-, $SO_4^{2-}-H_2O$ at 373 K [10] have been carried by our group.

It is generally known that the phase equilibria and phase diagrams are the theoretic foundation for the exploitation of underground brine resources. K.S. Pitzer published a series of papers about electrolyte solutions, and came up with a set of semi-empirical theory of statistical mechanics. It can be successfully applied to electrolyte solutions at high concentrations. A number of theoretical studies on salt minerals and brine system have been carried out in recent decades. Aiming at the seawater system, Harvie et al. carried out a series of research and extended the Pitzer ion-interaction model to Harvie–Weare (H–W) model in the prediction for the $Na-K-Mg-Ca-H-Cl-SO_4-OH-HCO_3-CO_3-CO_2-H_2O$ system at 25°C [11–13]. In order to increase the applicability to a number of diverse geochemical systems at higher or lower temperatures, additional work has centered on developing variable temperature models. Then, the $H-Na-K-Ca-OH-Cl-HSO_4-SO_4-H_2O$ system from zero to high concentration and temperature and natural waters $Na-K-Ca-Mg-Cl-H_2O$ system at temperatures below 25°C have been developed [14–18]. For the bromide-bearing brine system, Christov and co-workers develop a well validated and fully consistent model for $Li-Na-K-NH_4-Rb-Cs-Mg-Ca-Cl-Br-H_2O$ system at standard temperature [19–28]. In recent years, Christov have made a series of research work for bromide-rich brine system $Na-K-Mg-Ca-Br-SO_4-H_2O$ [29–34].

[1] The article is published in the original.

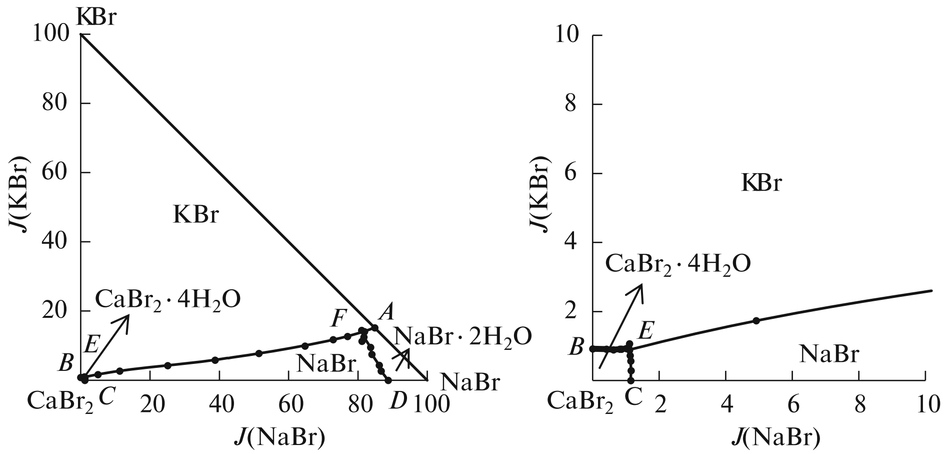

Fig. 1. Dry-salt solubility diagram and its enlarged bottom of quaternary system $NaBr-KBr-CaBr_2-H_2O$ at 323 K.

The quaternary system $NaBr-KBr-CaBr_2-H_2O$ is one subsystem of the brine-salt system in Western Sichuan Basin. This paper continues our studies concerning this quaternary system at 323 K, and the research work includes four parts: (1) measure the solubilities in the equilibrium solution for the quaternary system $NaBr-KBr-CaBr_2-H_2O$ at 323 K by isothermal method; (2) identify the equilibrium solid phases and give the experimental phase diagram of the system; (3) calculate solubilities in quaternary system $NaBr-KBr-CaBr_2-H_2O$ at 323 K with reasonable parameters, and compare calculated solubilities with experimental data.

EXPERIMENTAL

Reagents and Instruments

A standard analytical balance of 110 g capacity and 0.0001 g resolution (AL104), manufactured by the Mettler Toledo Instruments, was used. An HZS-H type thermostatic water bath shaker provided ±0.1 K accuracy when using precision thermometer calibration.

The chemicals used were of analytically pure grade. That is sodium bromide (NaBr, 99.0 wt %), potassium bromide (KBr, ≥99.0 wt %) (Chengdu Kelong Chemical Reagent Manufactory, China.), and calcium bromide dihydrate ($CaBr_2 \cdot 2H_2O$, ≥98.0 wt %) (Tianjin Guangfu Fine Chemical Research Institute, China.). The water used was distilled. Conductivity of the water is less than 1.2×10^{-4} S m^{-1}, with pH value 6.60 at room temperature.

Experimental Method

The phase equilibria in the quaternary system at 323 K were investigated using the isothermal dissolution equilibrium method. The system points of the quaternary system were prepared by adding the third salt component gradually on the basis of the ternary invariant points at 323 K. The prepared mixtures were placed in sealed glass bottles and dissolved into 50 mL of deionized water. In this way, all brine samples can be synthesized artificially. The bottles were then placed on a thermostatted water bath shaker (HZS-H). The sample temperature was maintained at 323 ± 0.1 K. The solutions were taken out periodically for chemical analysis. The criterion for judging the equilibrium state of the system was the unchanging concentration of the solution. After equilibrium settles, the solution and wet crystals were taken out for physicochemical analysis. The liquid phases were analyzed quantitatively by chemical methods, while the wet crystals were analyzed by X-ray diffraction to ascertain their crystalline form.

Analytical Methods

The Br^- ion concentration was analyzed by silver nitrate volumetric titration (uncertainty of 0.3%). The K^+ ion concentration was determined by a sodium tetraphenylborate (STPB)—hexadecyltrimethylammonium bromide (CTAB) titration (uncertainty of 0.5%). The Ca^{2+} ion concentration was determined by titration with EDTA standard solution in the presence of alkali and Ca-indicator (uncertainty of 0.3%). The Na^+ ion concentration was evaluated on an ion balance.

The experimental results of system $NaBr-KBr-CaBr_2-H_2O$ at 323 K are presented in Table 1, and the ion concentration values in the equilibrium solution are expressed as mass fraction. The solubility diagram of the quaternary system is expressed with Jänecke dry-salt indices, which can be defined as follows:

$$J(B) = 100\frac{w(\mathrm{B})}{w_s}, \tag{1}$$

Table 1. Solubilities of solution in the quaternary system $NaBr-KBr-CaBr_2-H_2O$ at 323 K

No.	Composition of liquid phase 100*w*(B)			Jänecke index *J*, g/100 g $J(NaBr) + J(KBr) + J(CaBr_2) = 100$ g				Equilibrium solids
	w(NaBr)	*w*(KBr)	$w(CaBr_2)$	*J*(NaBr)	*J*(KBr)	$J(CaBr_2)$	$J(H_2O)$	
1, A	48.12	8.61	0	84.82	15.18	0	76.29	NB2 + KB
2	46.92	8.11	2.29	81.86	14.15	3.99	74.45	NB2 + KB
3	44.95	7.40	6.01	77.02	12.69	10.30	71.33	NB + KB
4	43.19	7.02	9.12	72.80	11.84	15.36	68.54	NB + KB
5	39.73	6.12	15.53	64.72	9.98	25.30	62.93	NB + KB
6	32.87	4.98	26.05	51.43	7.80	40.77	56.49	NB + KB
7	25.63	3.91	36.54	38.78	5.91	55.31	51.35	NB + KB
8	17.00	2.91	47.80	25.11	4.30	70.60	47.69	NB + KB
9	7.79	1.90	59.86	11.20	2.73	86.07	43.77	NB + KB
10	3.45	1.22	65.40	4.92	1.74	93.34	42.72	NB + KB
11	0.79	0.63	69.97	1.11	0.89	98.01	40.08	NB + KB
12, C	0.81	0	69.97	1.15	0	98.85	41.29	NB + CB4
13	0.82	0.20	69.82	1.15	0.29	98.56	41.16	NB + CB4
14	0.81	0.40	69.55	1.14	0.57	98.29	41.32	NB + CB4
15	0.79	0.51	69.55	1.12	0.73	98.15	41.13	NB + CB4
16	0.79	0.76	69.87	1.11	1.07	97.83	40.02	NB + CB4
17	0.77	0.73	69.59	1.08	1.03	97.89	40.66	NB + CB4
18, B	0	0.65	70.49	0	0.92	99.08	40.55	CB4 + KB
19	0.30	0.65	70.30	0.41	0.91	98.67	40.36	CB4 + KB
20	0.44	0.64	70.30	0.62	0.89	98.49	40.10	CB4 + KB
21	0.59	0.66	71.03	0.82	0.91	98.27	38.36	CB4 + KB
22	0.62	0.65	70.71	0.87	0.91	98.23	38.91	CB4 + KB
23, E	0.72	0.67	70.22	1.01	0.93	98.06	39.65	NB + KB + CB4
24, D	47.08	0	5.99	88.71	0	11.29	88.44	NB + NB2
25	46.98	1.49	5.73	86.68	2.75	10.57	84.50	NB + NB2
26	46.80	2.38	5.14	86.15	4.38	9.47	84.10	NB + NB2
27	45.69	4.12	4.59	83.99	7.57	8.44	83.81	NB + NB2
28	45.85	5.31	4.23	82.77	9.59	7.64	80.50	NB + NB2
29	45.52	6.30	3.74	81.93	11.34	6.73	79.99	NB + NB2
30	45.77	7.03	3.22	81.71	12.55	5.74	78.52	NB + NB2
31, F	45.93	8.15	2.48	81.21	14.40	4.39	76.79	NB + NB2 + KB

w(B) is the mass fraction of component B.
Uncertainties: *T*, ±0.1 K; *w*(NaBr), ±0.5%; *w*(KBr), ±0.5%; $w(CaBr_2)$, ±0.3%.
Abbreviations: NB = NaBr, NB2 = $NaBr \cdot 2H_2O$, KB = KBr, CB_4 = $CaBr_2 \cdot 4H_2O$.

$$J(H_2O) = 100\frac{w(H_2O)}{w_s}, \quad (2)$$

$$w_s = w(NaBr) + w(KBr) + w(CaBr_2), \quad (3)$$

where subscript "s" means "all dry salts," and component B can be NaBr, KBr, $CaBr_2$, or H_2O.

Using the experimental results in Table 1, the phase diagram of the quaternary system at 323 K is shown in

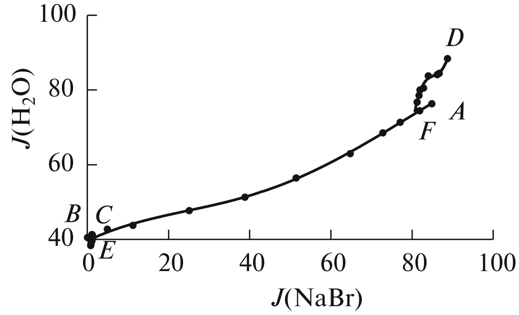

Fig. 2. Water contents of saturated solutions in quaternary system NaBr–KBr–$CaBr_2$–H_2O at 323 K.

Fig. 1 with solid lines. The phase diagram in Fig. 1 has four crystallization fields of single salts, five univariant curves, and two invariant points. Neither solid solutions nor double salts were found in quaternary system NaBr–KBr–$CaBr_2$–H_2O at 323 K. The saturated salts in the four crystallization fields are NaBr, NaBr · $2H_2O$, KBr, and $CaBr_2 \cdot 4H_2O$. The crystallization fields of single salt KBr is largest, whereas the crystallization fields of $CaBr_2 \cdot 4H_2O$ is smallest. These results indicate that the solubility of KBr in this quaternary system is very low, so it is easy to crystallize. The five-univariant solubility isotherm curves correspond to *BE*, *CE*, *EF*, *DF*, and *AF*. The invariant points of this quaternary system is labeled as *E* and *F*.

Invariant point *E*, saturated with salts $CaBr_2 \cdot 4H_2O$ + NaBr + KBr, with w(NaBr) = 0.0072, w(KBr) = 0.0067, and $w(CaBr_2)$ = 0.7022.

Invariant point *F*, saturated with salts NaBr · $2H_2O$ + NaBr + KBr, with w(NaBr) = 0.4593, w(KBr) = 0.0815, and $w(CaBr_2)$ = 0.0248.

The water diagram of the system NaBr–KBr–$CaBr_2$–H_2O at 323 K is shown in Fig. 2. The figure shows that Jänecke index of water of the quaternary system is changed regularly by the content change of sodium bromide and it reaches the maximum value at the point *D*.

Table 2. Pitzer single-salt parameters and Pitzer mixing ion-interaction parameters in the solution of the quaternary system NaBr–KBr–$CaBr_2$–H_2O at 323 K

Salt	$\beta^{(0)}$	$\beta^{(1)}$	C^{ϕ}	Reference
NaBr	0.130467	0.0842707	–0.004093	[29]
KBr	0.0648979	0.2651721	–0.002343	[29]
$CaBr_2$	0.3623529	2.1884234	0.0015618	[30]

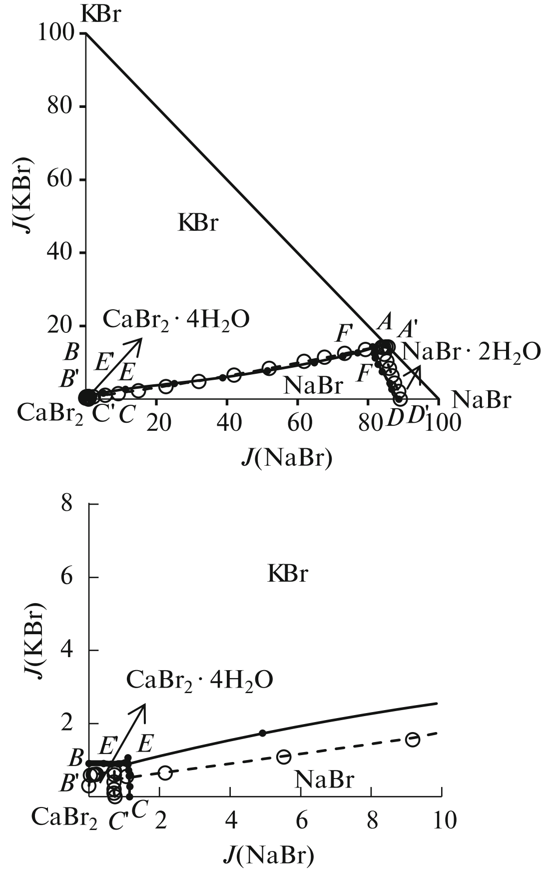

Fig. 3. The experimental and calculated phase diagram of the quaternary system NaBr–KBr–$CaBr_2$–H_2O at 323 K; —•—, experimental phase diagram; ···o···, calculated phase diagram.

PREDICTION OF SOLUBILITY

All the needed parameters for the system NaBr–KBr–$CaBr_2$–H_2O at 323 K can be obtained from literatures. The temperature dependent equation for the parameters is determined by adjusting selected constants in the following equation:

$$P(T) = a_1 + a_2T + a_3/T + a_4 \ln T + a_5/(T - 263) + a_6T^2 + a_7/(680 - T) + a_8/(T - 227) \quad (4)$$

where T is the Kelvin temperature. Debye–Hückel parameter A^{ϕ} and ln $K_w(\mu°/RT)$ H_2O(aq) at 323 K are available using this T-function given in T-variation model by Greenberg and Moller [15].

Christov [29, 30, 34] developed a bromide-rich T-variation model and it can provide the other needed Pitzer parameters for the system NaBr–KBr–$CaBr_2$–H_2O over temperatures ranging from 273.15 to 373.15 K. It was found that the constants a_3T^2, a_4T^3, $a_7/(T - 263)$, $a_8/(680 - T)$, and $a_9/(T - 227)$ in the model presented here are not necessary. Therefore, these are not included in the temperature dependence

Table 3. Values of Debye–Hückel constant (A^{ϕ}) and Pitzer mixing ion-interaction parameters in the solution of the quaternary system $NaBr–KBr–CaBr_2–H_2O$ at 323 K

Parameter	$\theta_{Na,K}$	$\theta_{Na,Ca}$	$\theta_{K,Ca}$	$\Psi_{Na,K,Br}$	$\Psi_{Na,Ca,Br}$	$\Psi_{K,Ca,Br}$	A^{ϕ}
Value	–0.006842	0.05	0.1156	–0.002042	–0.01899	–0.028	0.4103298
Reference	[15]	[30]	[34]	[29]	[30]	[34]	[15]

Table 4. Stable solubility constants of salts of the quaternary system $NaBr–KBr–CaBr_2–H_2O$ at 323 K

Salt	$\ln K_a$	Reference
NaBr	6.5470979	[29]
KBr	3.0893892	[29]
$CaBr_2 \cdot 4H_2O$	19.36726	[30]
$NaBr \cdot 2H_2O$	5.133012	[29]

Table 5. Calculated values of solution solubilities in the quaternary system $NaBr–KBr–CaBr_2–H_2O$ at 323 K

No.	Composition of liquid phase M, mol kg^{-1}				Jänecke index J, g/100 g $J(NaBr) + J(KBr) + J(CaBr_2) = 100$ g				Equilibrium solids
	$M(Na^+)$	$M(K^+)$	$M(Ca^{2+})$	$M(Br^-)$	$J(NaBr)$	$J(KBr)$	$J(CaBr_2)$	$J(H_2O)$	
1, B'	0	0.06	11.98	24.02	0	0.30	99.70	41.65	CB4 + KB
2	0.01	0.12	12.18	24.49	0.04	0.59	99.36	40.83	CB4 + KB
3	0.03	0.12	12.21	24.57	0.13	0.60	99.27	40.69	CB4 + KB
4	0.04	0.13	12.22	24.61	0.17	0.61	99.22	40.62	CB4 + KB
5	0.05	0.13	12.24	24.66	0.21	0.61	99.18	40.55	CB4 + KB
6	0.18	0.13	12.41	25.12	0.72	0.60	98.68	39.79	NB + CB4
7	0.17	0.08	12.32	24.89	0.71	0.40	98.88	40.18	NB + CB4
8	0.17	0.04	12.23	24.67	0.71	0.20	99.08	40.55	NB + CB4
9	0.17	0.02	12.19	24.57	0.71	0.10	99.19	40.73	NB + CB4
10, C'	0.17	0	11.99	24.15	0.74	0	99.26	41.44	NB + CB4
11, E'	0.18	0.15	12.46	25.25	0.72	0.69	98.59	39.59	NB + KB + CB4
12	0.23	0.10	10.84	22.00	1.07	0.55	98.38	45.43	NB + KB
13	0.40	0.10	9.21	18.92	2.16	0.65	97.19	52.81	NB + KB
14	0.87	0.15	7.58	16.19	5.52	1.09	93.39	61.62	NB + KB
15	1.35	0.20	6.77	15.09	9.18	1.56	89.27	65.97	NB + KB
16	2.08	0.28	5.96	14.28	14.88	2.31	82.81	69.55	NB + KB
17	3.07	0.40	5.15	13.76	22.70	3.41	73.89	71.87	NB + KB
18	4.27	0.56	4.33	13.49	32.02	4.85	63.12	72.92	NB + KB
19	5.58	0.76	3.52	13.37	41.99	6.57	51.44	73.15	NB + KB
20	6.91	0.97	2.71	13.30	52.00	8.46	39.54	73.12	NB + KB
21	8.20	1.19	1.89	13.18	61.88	10.39	27.73	73.31	NB + KB
22	8.92	1.31	1.42	13.07	67.60	11.50	20.90	73.66	NB + KB
23	9.61	1.42	0.95	12.93	73.38	12.58	14.04	74.23	NB + KB
24	10.27	1.53	0.47	1.53	79.26	13.64	7.10	75.05	NB + KB
25	10.94	1.60	0.09	12.71	84.46	14.25	1.29	75.01	NB2 + KB
26	10.99	1.60	0.04	12.67	85.06	14.29	0.65	75.22	NB2 + KB
27, A'	11.04	1.60	0	12.64	85.67	14.33	0	75.42	NB2 + KB
28, F'	10.89	1.60	0.13	12.75	83.84	14.22	1.93	74.83	NB + NB2 + KB
29	10.91	1.37	0.20	12.70	84.62	12.30	3.08	75.35	NB + NB2
30	10.83	1.14	0.28	12.54	85.31	10.41	4.27	76.54	NB + NB2
31	10.75	0.91	0.35	12.37	86.03	8.47	5.51	77.77	NB + NB2
32	10.67	0.69	0.43	12.21	86.76	6.45	6.79	79.04	NB + NB2
33	10.58	0.46	0.50	12.05	87.52	4.37	8.11	80.37	NB + NB2
34	10.89	0.23	0.58	11.68	88.68	2.15	9.17	79.15	NB + NB2
35, D'	10.41	0	0.65	11.72	89.12	0	10.88	83.17	NB + NB2

Abbreviations: NB = NaBr, NB2 = $NaBr \cdot 2H_2O$, KB = KBr, CB4 = $CaBr_2 \cdot 4H_2O$.

Table 6. Calculated and partly experimental solubilities in the quaternary system $NaBr-KBr-CaBr_2-H_2O$ at 323 K

	Composition of liquid phase 100*w*(B)			Jänecke index *J*, g/100 g $J(NaBr) + J(KBr) + J(CaBr_2) = 100$ g			Equilibrium solids
	w(NaBr)	*w*(KBr)	$w(CaBr_2)$	*J*(NaBr)	*J*(KBr)	$J(CaBr_2)$	
Experimental A	48.12	8.61	0	84.82	15.18	0	NB2 + KB
Calculated A'	48.84	8.17	0	85.67	14.33	0	
Experimental B	0	0.65	70.49	0.00	0.92	99.08	CB4 + KB
Calculated B'	0	0.21	70.39	0.00	0.30	99.70	
Experimental C	0.81	0	69.97	1.15	0	98.85	NB + CB4
Calculated C'	0.52	0	70.18	0.74	0	99.26	
Experimental D	47.08	0	5.99	88.71	0	11.29	NB + NB2
Calculated D'	48.65	0	5.94	89.12	0	10.88	
Experimental E	0.72	0.67	70.22	1.01	0.93	98.06	NB + KB + CB4
Calculated E'	0.52	0.50	70.63	0.72	0.69	98.59	
Experimental F	45.93	8.15	2.48	81.21	14.40	4.39	NB + NB2 + KB
Calculated F'	47.96	8.14	1.10	83.84	14.22	1.93	

Abbreviations: NB = NaBr, NB2 = $NaBr \cdot 2H_2O$, KB = KBr, CB4 = $CaBr_2 \cdot 4H_2O$.

for bromide solution parameters and chemical potential of bromide solids. The temperature dependence equation is as follow:

$$P(T) = a_1 + a_2T + a_5/T + a_6\ln T. \quad (5)$$

The Pitzer single-salt parameters $\beta^{(0)}$, $\beta^{(1)}$, C^{ϕ} for NaBr, KBr, $CaBr_2$, Pitzer mixing ion-interaction parameters $\theta_{Na,K}$, $\theta_{Na,Ca}$, $\theta_{K,Ca}$, $\psi_{Na,K,Br}$, $\psi_{Na,Ca,Br}$, $\psi_{K,Ca,Br}$, and stable solubility constants ln *K* of salts $NaBr \cdot 2H_2O$, NaBr, KBr, $CaBr_2 \cdot 4H_2O$ at 323 K all can be obtained and were fitted in Tables 2–5, respectively.

Using the parameters reported in the literatures, the values of the predicted solubilities for the quaternary system $NaBr-KBr-CaBr_2-H_2O$ at 323 K were calculated by the Pitzer and its extended H-W model. According to the results, a comparison between the experimental and calculated phase diagram of the system at 323 K is plotted in Fig. 3. In the phase diagram, solid lines show experimental isotherm curves and dashed lines show calculated ones. Comparison between the calculated solubilities and the experimental results at boundary points *A*, *B, C, D* and invariant points *E* and *F* of the quaternary system $NaBr-KBr-CaBr_2-H_2O$ at 323 K are shown in Table 6, the results show that the experimental phase diagram and the calculated one are in good agreement. It means that the parameters fitted in this work are reliable.

CONCLUSIONS

The phase equilibria in the quaternary system $NaBr-KBr-CaBr_2-H_2O$ were investigated at 323 K. The results show that this system was the hydrate II type. The phase diagram of the quaternary system consists of two invariant points, five univariant curves and four crystallization regions corresponding to NaBr, $NaBr \cdot 2H_2O$, KBr, and $CaBr_2 \cdot 4H_2O$. The solubilities of the quaternary system $NaBr-KBr-CaBr_2-H_2O$ at 323 K were calculated with corresponding parameters. The comparison between the calculation data and the experiment data were made. The calculated values agree well with the experimental data. It also shows that reasonable parameters of the Pitzer model can be used in aqueous salt system $NaBr-KBr-CaBr_2-H_2O$ at 323 K.

ACKNOWLEDGMENT

This project was supported by the National Natural Science Foundation of China (grant nos. 41373062 and U1407108) and scientific research and innovation team in Universities of Sichuan Provincial Department of Education (15TD0009).

REFERENCES

1. Y. T. Lin, J. Salt Lake Res. **9,** 56 (2001).
2. Y. T. Lin, J. Salt Lake Res. **14,** 1 (2006).
3. S. H. Sang, H. A. Yin, S. J. Ni, and C. J. Zhang, J. Chengdu Univ. Tech. (Sci. Technol. Ed., China) **33,** 414 (2006).
4. X. Y. Zhao, S. H. Sang, and M. L. Sun, J. Salt Lake Res. **19,** 35 (2011).
5. S. H. Sang, T. R. Li, and Z. Cui, J. Salt Lake Res. **12,** 29 (2013).
6. R. Z. Cui, S. H. Sang, Y. X. Hu, and J. W. Hu, Acta Geol. Sin. **87,** 1668 (2014).
7. Z. L. Zhang, S. H. Sang, M. Li, and C. H. Hou, Chem. Eng. (China) **37,** 45 (2009).

8. F. M. Hu, S. H. Sang, Y. G. Zhang, and J. J. Zhang, J. Salt Chem. Ind. **41**, 12 (2012).
9. R. Z. Cui, S. H. Sang, D. W. Li, and Q. Z. Liu, CALPHAD **49**, 120 (2015).
10. R. Z. Cui, S. H. Sang, and Q. Liu, J. Chem. Eng. Data **61**, 444 (2016).
11. C. E. Harvie and J. H. Weare, Geochim. Cosmochim. Acta **44**, 981 (1980).
12. C. E. Harvie, H. P. Eugster, and J. H. Weare, Geochim. Cosmochim. Acta **46**, 1603 (1982).
13. C. E. Harvie, N. Moller, and J. H. Weare, Geochim. Cosmochim. Acta **48**, 723 (1984).
14. N. Moller, Geochim. Cosmochim. Acta **52**, 821 (1988).
15. J. P. Greenberg and N. Moller, Geochim. Cosmochim. Acta **53**, 2503 (1989).
16. C. Christov and N. Moller, Geochim. Cosmochim. Acta **68**, 1309 (2004).
17. C. Christov and N. Moller, Geochim. Cosmochim. Acta **68**, 3717 (2004).
18. R. J. Speneer, N. J. Moller, and H. Weare, Geochim. Cosmochim. Acta **54**, 575 (1990).
19. C. Balarew and C. Christov, C.R. Acad. Bulg. Sci. **45**, 49 (1992).
20. C. Balarew, C. Christov, S. Petrenko, and V. Valyashko, J. Solution Chem. **22**, 173 (1993).
21. C. Christov, C. Balarew, V. Valyashko, and S. Petrenko, J. Solution Chem. **23**, 595 (1994).
22. C. Christov, S. Petrenko, C. Balarew, and V. Valyashko, Monatsh. Chem. **125**, 1371 (1994).
23. C. Christov, J. Chem. Thermodyn. **27**, 1267 (1995).
24. C. Christov and C. Balarew, J. Solution Chem. **24**, 1171 (1995).
25. C. Christov, CALPHAD **20**, 501 (1996).
26. C. Christov, Coll. Czech. Chem. Commun. **61**, 1585 (1996).
27. C. Christov, J. Chem. Thermodyn. **37**, 1036 (2005).
28. C. Christov, S. Velikova, and K. Ivanova, J. Chem. Thermodyn. **32**, 1505 (2000).
29. C. Christov, Geochim. Cosmochim. Acta **71**, 3557 (2007).
30. C. Christov, CALPHAD **35**, 42 (2011).
31. C. Christov, J. Chem. Thermodyn. **43**, 344 (2011).
32. C. Christov, CALPHAD **36**, 71 (2012).
33. C. Christov, J. Chem. Thermodyn. **47**, 335 (2012).
34. C. Christov, J. Chem. Thermodyn. **55**, 7 (2012).